Examining Laminate Properties of 3D Printed Composite-Like Materials

Tyler Guertin

AE5432 Composite Materials Course Project

Professor Nikhil Karanjgaokar

12/09/2021

Worcester Polytechnic Institute

Aerospace Engineering Department

I. Introduction

Laminate macro-mechanics is a wide-ranged field which can be applied to many modern composite materials. While the laminate mechanics studied in micromechanics are often specifically applied to the use of composite materials which are manufactured in more mainstream methods, such as carbon fiber-epoxy layup or injection molding, analyses can also be applied to materials produced through Fused-Fiber Fabrication (FFF) 3D printing. In FFF 3D printing, layers of thermoset polymer strands are set on a build plate with a set layer thickness and orientation, which can produce a continuous laminated structure with varying or constant cross section. Since these layers can be produced with layer orientation and thickness in mind, specifically designed 3D printed materials can be assumed to be orthotropic and follow similar micromechanical models to typical composites whether they are one material, or multi-material (composite) structures. Composite 3D Printed materials can come in several forms, such as short-fiber reinforced filaments and long-fiber reinforced filaments, both of which can be used to enhance properties of a typical one-material thermoset specimen. A one-material 3D printed specimen which is produced as an angle-oriented laminate at each layer will follow the same constitutive equation as any other composite, with separate properties being represented along the fiber of the filament and transverse to the filament direction. Likewise, with composite 3D printed materials that employ short fiber reinforcement, each layer can be modeled as an angle-oriented lamina, which has the unique property of producing a fiber reinforced fiber. This fiber—reinforced fiber is created due to the nature of 3D prints, which often do not fuse together fully, leaving voids between the cylindrical fibers. These voids can cause bigger problems in larger layer heights, with implications on both strength as well as the moisture content retention and thermal properties. Considerations can also be made on 3D printed materials with the use of certain failure criterion, such as the Puck-Schurmann relations, which will be reviewed in depth for used on both typical composites and extended for use with 3D printed composite specimens. As these relations are directly attributed to some 3D printed composites, it can be assumed that a single-material 3D print could also be applied if it satisfies the constitutive relation of laminate composites, this mostly being because of the similarities between the strictures of these materials made in FFF.

II. Relating Composite Mechanics to 3D Printed Specimens

When a 3D printed material of any kind, that being composite or non-composite, it can be produced in a fashion that has a consistent layer height, along with this, if a 100% infill pattern is chosen, different angles can be printed for each layer, creating a structure that can be optimized like that of a composite material, and of course, this method can also be used for 3D printing composite materials through either dual extrusion or short fiber reinforcements. For the sake of this paper, only 3D printed composite materials will be examined. The constitutive equation for orthotropic materials is defined in Equations (1) and (2) as the stress-strain relation and the strain-stress relation respectively. These relations employ the use of the stiffness matrix C, which notes stiffness values for each direction in the 3D space, and the compliance matrix S, which

$$\{\sigma\} = [C]\{\varepsilon\} \quad (1)$$

Equation 1: Stress-strain relation in terms of stiffness C

$$[S]\{\sigma\} = \{\varepsilon\} \quad (2)$$

Equation2: Strain-stress relation in terms of the compliance S

notes inverse values for compliance. The main caveat with this method of relation for 3D printing is that the midplane of the laminate must be perpendicular to the build direction for no cross-section variation. As shown in Figure 1 from [1], build orientation A would have to be broken into 3 separate constitutively related beams since the two C-clamp sections have a different cross section and are not continuous when analyzed using layer angles. This is contrary to build orientation B, where there is not variation in cross section, and each "lamina" remains the same and perpendicular to the lamina midplane. If cross section remains constant, such as with a rectangular prism, then the constitutive equation can be applied for all build directions and angle orientations. The above equations can also be applied for any lamina angle, hence, these equations have been written in terms of the 1, 2, 3 coordinate system, which must be deduced from the 0 degree coordinate system in X, Y, and Z. Since each layer can be assumed to be a fraction of a

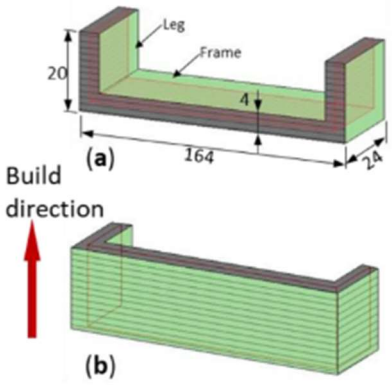

FIGURE 1: BUILD ORIENTATIONS AFFECTING LAMINA PROPERTIES IN 3D PRINTED SPECIMENS

millimeter for a typical 3D printed laminate, the constitutive relation is rewritten for a thin orthotropic layer in terms of the reduced stiffness matrix [1] in equation 3. This simplification can be written since the S13, S24, S42, and S41 terms are all zero, and since each diagonal defined below for S compliance (4) is the same, due to the relatively small thickness in a macroscopic sense, which employs a plane stress condition.

$$\{\sigma\} = [Q]\{\varepsilon\} \quad (3)$$

Equation 3: Stress-Strain relation when reduced to plane stress in terms of Q

$$S_{11} = \frac{1}{E_1}, S_{12} = -\frac{\nu_{12}}{E_2}, S_{13} = -\frac{\nu_{13}}{E_1}, S_{22} = \frac{1}{E_2}, S_{23} = -\frac{\nu_{23}}{E_2},$$
$$S_{33} = \frac{1}{E_3}, S_{44} = \frac{1}{G_{12}}, S_{55} = \frac{1}{G_{13}}, S_{66} = \frac{1}{G_{23}} \quad (4)$$

Equation 4: Compliance matrix equations for each direction, depends on poisons ratio and modulus of elasticity.

The consituitive relations above are all brought into the X, Y, Z coordinate space using the Q bar matrix, this is important to determine the properties in terms of each laminate orientation, which would all have different 1, 2, and 3 directions. By moving all of the above into the global coordinate system analysis become much easier. This new constitutive equation is written as equation 5.

$$[Q_{bar}] = [T]^{-1}[Q][T]^{-T} \quad (5)$$

Equation 5; Q bar reduced transformed stiffness matrix

$$\{\sigma\} = [Q_{bar}]\{\varepsilon\} \quad (6)$$

Equation 6: Stiffness relation in the XYZ space defined by the transformed reduced stiffness Q bar

This final relation achieved can be easily applied to find the stress in different directions in the XYZ space. This allows for typical laminate mechanical analysis on any part, and can be very useful for creating a strong specimen. This has many implications on both the stiffness and the strength of 3D printed materials that are both composites and non-composites.

III. Examination of various properties

There are many properties that can be examined when looking at any composite material, or material in general for that matter. Some are more prevalent than others, but due to the nature of 3D prints in terms of the randomness of voids in 3D printing, the examination of strain due to moisture and failure mechanics will be discussed. While these are unrelated in their respective senses, the implications of each on 3D prints is critical, and both prove to be extensions of the previous assumption that 3D printed materials printed in specific fashion can all be modeled by classical laminate theory and other standard composite analysis methods.

III.a Laminate Orientation in 3D Prints

The most fascinating thing about employing the above relations for any 3D printed material is it's implications on using layer orientation to strengthen 3D prints. Most 3D printed materials are seen as proof of concept or prototyping materials. Being able to construct a print in a fashion that maximizes strength increases the practicality of FFF printing by a lot. This is specifically true for design of parts that need a high flexural stiffness. ABS non-composite materials printed using FFF methods were modeled using the constitutive equation and printed at angle ply and cross ply orientations to determine structural capabilities using a 3-point bending test. This was done using 3 different symmetrical build orientations, allowing for laminate mechanics to be applied to each beam in a different fashion (with different cross section). One consideration to be made with such analysis is that when modeling 3D prints, properties are much harder to replicate in experiments due to the presence of internal voids between layers and fibers [4]. As well as this, due to the quality produced by varying FFF machines, many other defects can occur to affect laminate properties.

Typically, an angle ply-laminate will have good flexural properties, as it is of the form [Theta/ -Theta], which will thus produce properties that do not promote torsional movement. This is due to the "replication" of properties essentially reflected over the midplane axis (in this specific case) [5]. As for cross ply laminates, they are usually used

in applications which can be used both for flexural stiffness as well as protection from crack mitigation (due to harsh angle turn). Also, since these laminates only employ 0- and 90-degree angles, Q_16 and Q_26 are zero, indicating that these laminates are “specially orthotropic” [7].

The affect of this angle orientation on purely ABS prints is shown below from [1]. Analyzing the graph shows that the strongest flexural properties were concentrated in the angle-ply laminates, which is to be expected via the discussion above. Cross-ply ABS laminates appeared to be stiffer under flexural loads, but only by very small amounts. Upright printing resulted in failure the most easily, most likely due to the small cross section and high number of laminates. Since there was a high number of laminates in that build orientation, there is much better chance of delamination between layers. This can be compared to a carbon-fiber epoxy laminate, which are generally of larger cross section in the laminate plane.

All the points discussed previously confirm the similarity of the actions of composite laminates to that of a one-material 3D printed laminate structure. This can also be seen when comparing the second figure below, which employs a continuous long-fiber 3D printed composite called ABS-SCF in similar orientations. This composite is modeled as a thermoset matrix with magnesium short fibers added into the filament. This is frequently done with many materials to enhance filament properties.

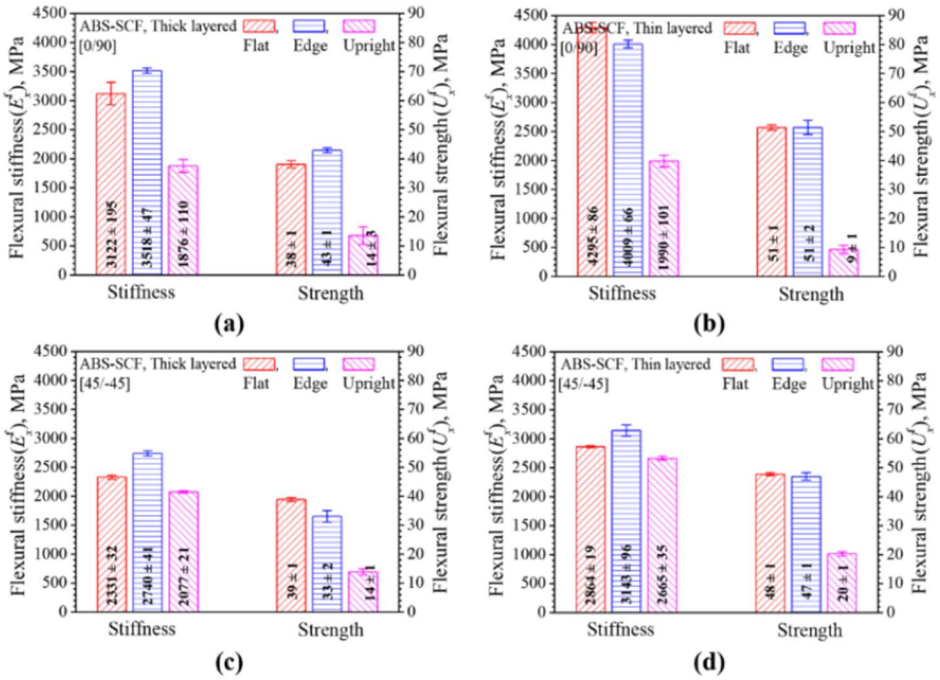

Figure 1: Flexural Properties of experimental 3D printed ABS angle-oriented laminates [1]

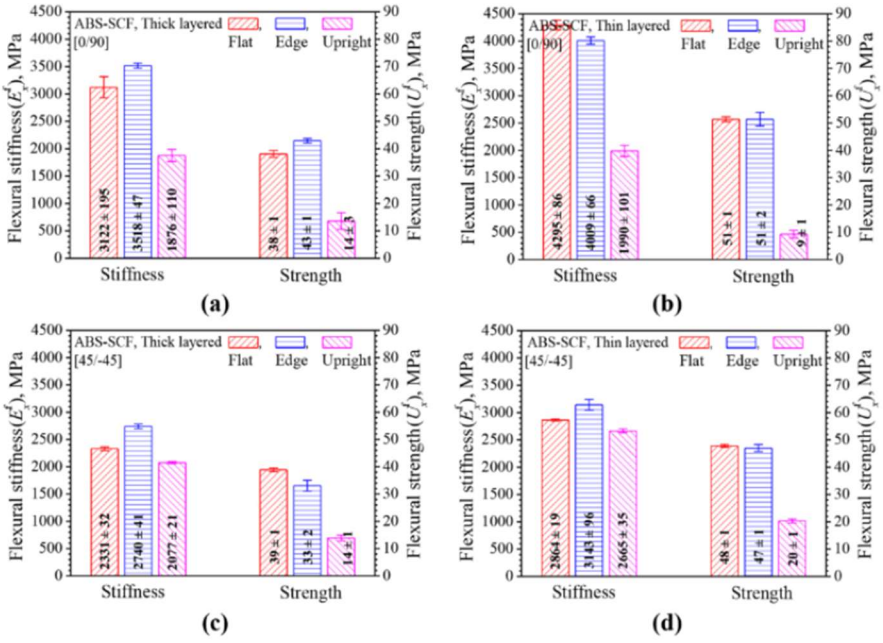

Figure 2: Flexural properties of experimental 3D printed ABS-SCF angle-oriented laminates [1]

III.b Moisture retention

While the last discussion was primarily based on similarity to composite materials of single-material 3D prints, this section will focus primarily on the properties of 3D printed materials (composites) having to do with moisture retention. As mentioned in the previous section, thin layers are used in most 3D printed materials, and due to the nature of 3D printing voids must be considered more prevalently than in other manufacturing methods. While the first instinct could be to think that these voids could cause the most problems in the sense of strength and stiffness, expansion due to moisture is also an important consideration, especially when considering composite materials, as this may deteriorate the fiber and matrix properties individually. A specific example of this special case would be in a short-fiber reinforced wood PLA. This filament contains a thermoset matrix with wood flakes put in to simulate properties and look of wood. This is a good example of a 3D printed material that could be produced with layer orientation to employ CLT for a short-fiber matrix (since that is usually applied to a continuous fiber matrix). As it is known, the strain due to moisture can be written in the form of equation (7). This simple relation can be applied to the figure below as well, which notes experimental data from 28 days of moisture absorption 3D printed structures made from wood PLA with [0/0/0/0] orientation, and varying lamina thickness [2].

$$\{\varepsilon\}_{123} = \{\beta\}_{123} * \Delta M \quad (7)$$

Equation 7: Definition of strain due to moisture in an orthotropic material

Table 1 Water absorption and mechanical properties of 3D-printed wood/PLA composite samples

3D-printed wood/PLA sample code	Printing layer thickness (mm)	Density (g/cm)	Water absorption (28 days) (%)	Bending properties		Tensile properties	
				Bending strength (MPa)	Bending modulus (MPa)	Tensile strength (MPa)	Tensile modulus (MPa)
A	0.05	1.008 (0.010)	0.19 (0.03) a	128.3 (4.0) a	4887 (145) a	35.5 (1.5) a	3642 (122) a
B	0.1	0.993 (0.011)	0.22 (0.05) a	121.7 (4.2) b	4350 (125) b	33.9 (1.2) b	3410 (141) b
C	0.2	0.980 (0.009)	0.64 (0.04) b	113.6 (3.8) c	4125 (137) c	28.7 (1.4) c	3115 (133) c
D	0.3	0.975 (0.08)	0.72 (0.06) c	84.3 (2.8) d	3580 (103) d	20.5 (0.7) d	2567 (92) d

Groups with the same letters in a column indicate that there is no statistical difference ($p < 0.05$) between the specimens according to Duncan's multiple range test. The values in the parentheses are standard deviations

Figure 3: Table of water absorption affected properties after 28 days in layered wood PLA specimens [2]

It is important to note how the properties change with respect to layer thickness, and also how the material properties may differ from the use of pure PLA rather than the wood PLA being tested. Generally, from the data, with all parameters repeated for each specimen of different

laminate thickness, the thinnest laminae had the best properties [2]. This could be postulated due to poor layer adhesion of each lamina with a larger thickness, or perhaps due to more space for water penetration stemming from voids in the material. Relating this the the CLT constitutive equation for stress and strain, it is important to note that train values directly depend on the thickness of each layer, so in that sense, the stress in the smallest layer height would be largest. Of course, this does not account for the two considerations of the water absorption and the presence of voids mentioned above. In this scope, it is interesting to compare how the water absorption due to voids has affected the strength of the thicker composite structure so negatively.

III.c Failure Modes

The failure of materials is always an important consideration in mechanics, and this is no different for with 3D printed materials. There are many models for failure of composite materials in a general sense, however, by extending the Puck and Shurmann relations for fiber-reinforced composite materials [3], failure criteria can be determined.

In comparison to more classical methods in composite mechanics such as the Tsai-Hill theory or the Tsai-Wu theory, the Puck and Schurmann failure envelope extends upon Mohr-Coulomb relations (similar to Mohr's circle) and applies to the different angled planes rotated around a continuous fiber axis. The interesting thing about this method is that it shows the dependence of failure on both the shear and normal stresses in a plane, and accounts for the relationship between those stresses though the slope of their relative graphs, these terms being p_{ψ}^{t} and other p terms. This provides a direct relation between each normal force and the two shear forces on a given plane, which are calculated for failure analysis from -90 to 90 degrees via the equations mentioned in Figure 5. This analysis domain allows the failure envelope to be reflected across the axis for negative values of shear stress and the equivalent values of the

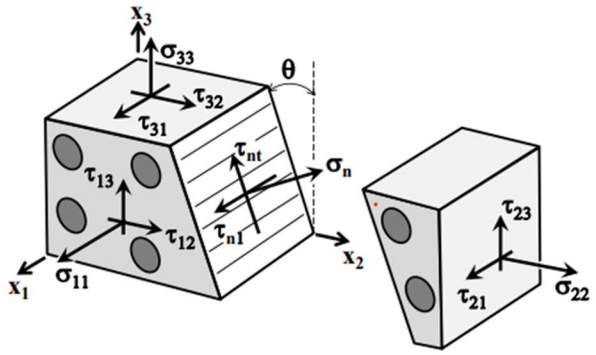

FIGURE 4: ILLUSTRATION OF FRACTURE PLANE ANALYSIS FOR FIBER-REINFORCED COMPOSITES AROUND THE FIBER AXIS

$$\sigma_n(\theta) = \sigma_{22}\cos^2(\theta) + \sigma_{33}\sin^2(\theta) + 2\tau_{23}\sin(\theta)\cos(\theta),$$
$$\tau_{nt}(\theta) = -\sigma_{22}\sin(\theta)\cos(\theta) + \sigma_{33}\sin(\theta)\cos(\theta) + \tau_{23}\left[\cos^2(\theta) - \sin^2(\theta)\right]$$
$$\tau_{n1}(\theta) = \tau_{13}\sin(\theta) + \tau_{12}\cos(\theta).$$

FIGURE 5: EQUATIONS FOR DETERMINING STRESS HOUSED WITHIN A SPECIFIC PLANE FROM ANGLE -90 TO 90

normal stress for a given angle. Of course, like the theories discussed above, the compressive strength and shear strength are still important considering factors for fracture to occur in a given plane. When the fracture condition in Figure 7 is satisfied, the envelope becomes "closed" at that point. Since for this theory, both shear and normal are combined in analysis, but two different conditions are defined when the normal stress is positive and negative [3][6], this has to do with the compressive and tensile properties within the composite under differing loads. In Figure 6, the fracture mechanisms of a thermoset matrix composite is shown. Mode A occurs where there is pure normal stress, while Mode B occurs where there is pure shear stress. From here, the envelope must be applied until the condition reaches where $R^a_{\perp\perp}$ is equal to the normal stress. Both mode A and B are held at a zero-degree angle, and the function is defined in a piecewise nature for this condition where the normal force is above and below 0. Mode C is the final value calculated, which constitutes failure at the negative most value of the normal force. All of the in between values for these failure conditions have to be checked for every angle between 0 and 90 for failure, which is tedious, but produces an accurate envelope.

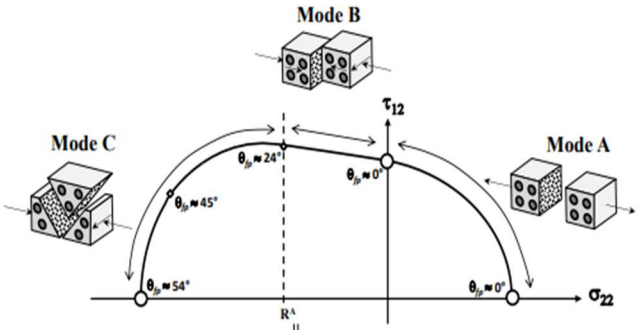

FIGURE 6: ILLUSTRATION OF THE FAILURE ENVELOPE FOR FIBER-REINFORCED COMPOSITES (NON 3D PRINTED)

The envelope does not quite line up when calculated for a thermoset matrix composite, this could be because the original Puck-Schurmann fracture criteria were designed for particularly brittle materials [3][6]. The glass-fiber 3D printed composite considered in [3] produced a 3D relation that was applicable, however Modes A and B did follow experimental values for failure, making the model at least partially correct. To fully correct the situation for any 3D printed composite, a new mode was created and labeled as Mode BB. This mode considers the slope of the normal force vs. tangential shear. This parameter is not specific, but it should be noted that Mode BB corresponds a zero value of the normal force up to 2 $R^a_{\perp\perp}$, which extended the B mode beyond a pure 0-degree condition. This also assumes that all normal vs shear relations have the same inclination parameters. Lastly, it is important to note that the paper assumes that a 2D stress state is acting over a 3D printed composite material [3]. This means that

the 3D relation that fits the criteria with no discontinuities can be applied and thus the criteria is "extended".

$$f_E(\theta) = \sqrt{\left[\left(\frac{1}{R_\perp^A} - \frac{p_{\perp\psi}^t}{R_{\perp\psi}^A}\right)\sigma_n(\theta)\right]^2 + \left[\frac{\tau_{nt}(\theta)}{R_{\perp\perp}^A}\right]^2 + \left[\frac{\tau_{n1}(\theta)}{R_{\perp\parallel}^A}\right]^2} + \frac{p_{\perp\psi}^t}{R_{\perp\psi}^A}\sigma_n(\theta), \text{ for } \sigma_n(\theta) \geq 0, \quad (2a)$$

$$f_E(\theta) = \sqrt{\left[\frac{p_{\perp\psi}^c}{R_{\perp\psi}^A}\sigma_n(\theta)\right]^2 + \left[\frac{\tau_{nt}(\theta)}{R_{\perp\perp}^A}\right]^2 + \left[\frac{\tau_{n1}(\theta)}{R_{\perp\parallel}^A}\right]^2} + \frac{p_{\perp\psi}^c}{R_{\perp\psi}^A}\sigma_n(\theta), \text{ for } \sigma_n(\theta) < 0, \quad (2b)$$

with

$$\frac{p_{\perp\psi}^{t,c}}{R_{\perp\psi}^A} = \frac{p_{\perp\perp}^{t,c}}{R_{\perp\perp}^A}\cos^2\psi + \frac{p_{\perp\parallel}^{t,c}}{R_{\perp\parallel}^A}\sin^2\psi, \quad (3a)$$

$$\cos^2\psi = \frac{\tau_{nt}^2}{\tau_{nt}^2 + \tau_{n1}^2}, \quad (3b)$$

$$\sin^2\psi = \frac{\tau_{n1}^2}{\tau_{nt}^2 + \tau_{n1}^2}, \quad (3c)$$

$$R_{\perp\perp}^A = \frac{R_\perp^c}{2\left(1 + p_{\perp\perp}^c\right)}, \quad (3d)$$

$$R_\perp^c = Y_C, \quad (3e)$$

$$R_\perp^A = R_\perp^t = Y_T, \quad (3f)$$

$$R_{\perp\parallel}^A = S_{12}, \quad (3g)$$

Figure 7: The above relation is the fracture condition for the Puck-Schurmann relation

IV. Conclusion

Composite mechanics are successfully applied to 3D printing in a variety of sub-disciplines and can be very useful for the analysis of both 3D printed materials and 3D printed composites in general. The relations discussed here only scratch the surface of several of the ideas that can be equally applied between these two overlapping material groups. It is important to note that among these methods, many discrepancies may be seen, as very specific conditions must be met for the application of some more advanced criteria, such as Puck and Shurmann, which is amended above for specific use on non-brittle materials. The overall consensus of this conclusion is to inform that while the methods above are representative in their specific means, they are only a representation of the possible relations to the FFF 3D-Printing method for producing 3D printed materials and composites. The ability to apply the constitutive equation for composite laminate to 3D prints allows for a new world of analysis to be examined in 3D printing, and for a more practical use for 3D printed composites to be developed. The continuation of research into 3D printed composites and their properties will redefine the way that 3D printing is seen and make way for cheap and accessible use of durable and strong, easily manufactured materials.

V. References

[1] Somireddy, M. Czekanski, A. Anisotropic Behavior of 3D Printed Composite structures – Material extrusion additive manufacturing, *Materials and Design 195 (2020)*

[2] Ayrilmis, N. Kariz, M. Kwon, J.H. Kuzman, M.K. Effect of printing layer thickness on water absorption and mechanical properties of 3D-printed wood/PLA composite materials, *Journal of Advanced Manufacturing Technology (2019)*

[3] Thiago Assis Dutra; Rafael Thiago Luiz Ferreira; Hugo Borelli Resende; Blinzler, Brina Jane; Larsson, Ragnar, Expanding Puck and Schurmann Inter Fiber Fracture Criterion for Fiber Reinforced Thermoplastic 3D-Printed Composite Materials*; Basel Vol. 13, Iss. 7, (2020): p. 1653*

[4] M. Somireddy, C.V. Singh, A. Czekanski, Mechanical behaviour of 3D printed composite parts with short carbon fiber reinforcements, *Engineering Failure Analysis, Volume 107, 2020*

[5] George H. Staab, 6 - Laminate analysis*, Editor(s): George H. Staab, Laminar Composites (Second Edition), Butterworth-Heinemann, 2015, Pages 189-284*

[6] A. Puck, H. Schurmann, *Failure analysis of FRP laminates by means of physically based phenomenological models, Composites Science and Technology, Volume 62, Issues 12–13, 2002, Pages 1633-1662*